



# Equilibrium thallium isotope fractionation and its constraint on Earth's late veneer

Tong Fang<sup>1,2</sup> · Yun Liu<sup>1,3</sup>

Received: 13 April 2019 / Revised: 25 April 2019 / Accepted: 25 April 2019 / Published online: 14 May 2019  
© Science Press and Institute of Geochemistry, CAS and Springer-Verlag GmbH Germany, part of Springer Nature 2019

**Abstract** Equilibrium isotope fractionation of thallium (Tl) includes the traditional mass-dependent isotope fractionation effect and the nuclear volume effect (NVE). The NVE dominates the overall isotope fractionation, especially at high temperatures. Heavy Tl isotopes tend to be enriched in oxidized  $Tl^{3+}$ -bearing species. Our NVE fractionation results of oxidizing  $Tl^+$  to  $Tl^{3+}$  can explain the positive enrichments observed in ferromanganese sediments. Experimental results indicate that there could be 0.2–0.3  $\epsilon$ -unit fractionation between sulfides and silicates at 1650 °C. It is consistent with our calculation results, which are in the range of 0.17–0.38  $\epsilon$ -unit. Importantly, Tl's concentration in the bulk silicate Earth (BSE) can be used to constrain the amount of materials delivered to Earth during the late veneer accretion stage. Because the Tl concentration in BSE is very low and its Tl isotope composition is similar with that of chondrites, suggesting either no Tl isotope fractionation occurred during numerous evaporation events, or the Tl in current BSE was totally delivered by late veneer. If it is the latter, the Tl-content-based estimation could challenge the magnitude of late veneer which had been constrained by the amount of highly siderophile elements in BSE. Our results show that the late-

accreted mass is at least five-times larger than the previously suggested magnitude, i.e., 0.5 wt% of current Earth's mass. The slightly lighter  $^{205}Tl$  composition of BSE relative to chondrites is probable a sign of occurrence of Tl-bearing sulfides, which probably were removed from the mantle in the last accretion stage of the Earth.

**Keywords** Equilibrium Tl isotope fractionation · Nuclear volume effect · Tl fractionations between silicates and sulfides · Late veneer · First-principles calculation

## 1 Introduction

The thallium (Tl) isotope system has been used as a high-precision tool to trace geologic processes since the techniques used to measure Tl isotope ratio became enhanced in 1999 (Rehkamper and Halliday 1999). Tl is a lithophile and chalcophile element (Shaw 1952; McGoldrick et al. 1979; Wood et al. 2008), and as such it is present in both silicate and sulfide phases. The knowledge of elemental partition and isotope fractionation for Tl is vitally essential for Tl to be used as tracers in the study of the Earth's differentiation processes. Tl is likely to enter the metal core if a sulfide phase exists, causing Tl to undergo elemental partition and isotope fractionations during core-mantle differentiation (Wood et al. 2008). Hence, the Tl isotope fractionation factors of the coexisting phases between silicates and sulfides are very important to deciphering the magmatic evolution in the accretion stage of Earth.

Tl behaves as an incompatible element during the process of magmatic crystallization and differentiation (Shaw 1952).  $Tl^+$  ion can be replaced by the ions of alkali metal, such as  $K^+$  and  $Rb^+$ , in phyllosilicate and feldspar minerals (Shaw 1952; Heinrichs et al. 1980). Thallium is a highly

✉ Yun Liu  
liuyun@vip.gyig.ac.cn

<sup>1</sup> State Key Laboratory of Ore Deposit Geochemistry, Institute of Geochemistry, Chinese Academy of Sciences, Guiyang 550081, People's Republic of China

<sup>2</sup> University of Chinese Academy of Sciences, No. 19(A) Yuquan Road, Shijingshan District, Beijing 100049, People's Republic of China

<sup>3</sup> CAS Center for Excellence in Comparative Planetology, Hefei, People's Republic of China

volatile element; its equilibrium condensation temperature is 532 K in the form of troilite ( $\text{Tl}_2\text{S}$ ,  $\text{Tl}_2\text{Se}$ ,  $\text{Tl}_2\text{Te}$ ) (Lodders 2003). During the processes of evaporation and condensation in the accretion of Earth, the loss or migration of Tl could result in stable Tl isotope fractionation in addition to possible dynamic fractionation. We can use the first-principles calculation to estimate such equilibrium Tl isotope fractionations.

Thallium has two isotopes in nature, i.e.,  $^{203}\text{Tl}$  (29.5%) and  $^{205}\text{Tl}$  (70.5%). The isotope fractionation factor of Tl isotopes,  $\epsilon^{205}\text{Tl}$ , denotes the deviation of  $^{205}\text{Tl}/^{203}\text{Tl}$  in parts per 10,000 relative to the standard sample (NIST SRM 997 Tl metal). The variation of  $\epsilon^{205}\text{Tl}$  for terrestrial samples is more than 35  $\epsilon^{205}\text{Tl}$ . The largest fractionation was observed between the low temperature altered oceanic crust ( $-20 \epsilon^{205}\text{Tl}$ ) and Fe–Mn sediments ( $+15 \epsilon^{205}\text{Tl}$ ) (Rehkamper et al. 2002; Nielsen et al. 2006b, 2013, 2015). Various meteorites have been shown to exhibit a wide range, with variations even as high as 50  $\epsilon^{205}\text{Tl}$  (Nielsen et al. 2006a; Andreasen et al. 2009; Palk et al. 2011; Nielsen et al. 2017). The  $\epsilon^{205}\text{Tl}$  of an outlier for carbonaceous chondrites is about 5.2, ranged from  $-4$  to  $+1.2$ , which is proportional to the ratio of Pb/Tl (Baker et al. 2010). This relationship results from the decay of  $^{205}\text{Pb}$  to  $^{205}\text{Tl}$  and the differentiation of Pb/Tl in the early solar system (Baker et al. 2010). The composition of  $\epsilon^{205}\text{Tl}$  for ordinary chondrites ranges from  $-20$  to  $+15$ , and this large fractionation is probably caused by the thermal metamorphism (Andreasen et al. 2009). Enstatite chondrites exhibits  $\epsilon^{205}\text{Tl}$  values ranging from  $-2.9$  to  $+0.8$  (Palk et al. 2011). For iron meteorites,  $\epsilon^{205}\text{Tl}$  exhibits an extremely large variation spanning about 50  $\epsilon$  ( $-19$  to  $+30$ ) (Nielsen et al. 2006a; Andreasen et al. 2009). The maximal variation of  $\epsilon^{205}\text{Tl}$  is believed to be produced by the decay of  $^{205}\text{Pb}$  under different environments with different Pb/Tl ratio. Another explanation is the kinetic isotope effect of stable isotope fractionation on  $^{205}\text{Tl}/^{203}\text{Tl}$  during the process of evaporation and condensation (Nielsen et al. 2006a). The  $^{205}\text{Pb}$ – $^{205}\text{Tl}$  system can be a promising tool for dating the early solar system events with a short half-life of 15.1 Ma (Pengra et al. 1978). It is believed that the extinct nuclide  $^{205}\text{Pb}$  was formed by the nucleosynthesis s-process (Yokoi et al. 1985). The initial composition of  $^{205}\text{Pb}$  of the solar system was determined by isochronal dating method using a group of carbonaceous chondrites (Baker et al. 2010).

The average  $\epsilon^{205}\text{Tl}$  in the bulk silicate Earth (BSE) is around  $-2$ , similar to that in continental crust and Mid-ocean ridge basalt (MORB) (Nielsen et al. 2005, 2006b, 2007). The variation in  $\epsilon^{205}\text{Tl}$  among natural terrestrial samples is measurable, and the fractionations were proved to be considerable, ranging from  $-20$  to  $+15 \epsilon^{205}\text{Tl}$  (Rader et al. 2018). Moreover, sulfide minerals

contain the heaviest Tl isotope signals, and Fe-rich micas show the minor value of  $\epsilon^{205}\text{Tl}$  (Rader et al. 2018). In high-pressure and high-temperature experiments, the Tl isotope fractionation between the silicate and sulfide reached to  $0.2$ – $0.3 \epsilon^{205}\text{Tl}$  and the fractionation between the silicate and the metal reached  $1.1 \epsilon^{205}\text{Tl}$  at about  $1650 \text{ }^\circ\text{C}$  (Wood et al. 2008). The reason for Tl isotope fractionations at such high temperatures has not been carefully investigated yet.

The relative mass difference of thallium's two isotopes is tiny. Therefore, it is likely that the mass-dependence fractionation contribution is a secondary factor for the overall equilibrium Tl isotope fractionation (Bigeleisen 1996; Fujii et al. 2013; Moynier et al. 2013). Tl is a heavy metal element with an atomic number of 81. Thallium exists mostly as Tl(I) in nature, but under an extremely oxidized condition or in surface environments Tl can exist as Tl(III) (Nielsen et al. 2017; Rader et al. 2018). There is a difference of two s electrons between two oxidation states. Therefore, considerable contributions of Tl isotope fractionation could be brought by the nuclear volume effect (NVE) (Schauble 2007; Nielsen 2011; Fujii et al. 2013; Moynier et al. 2013; Hettmann et al. 2014; Yang and Liu 2015). The directions of both mass-dependent and NVE-driven stable isotope fractionations are the same. The oxidized species (Tl(III)) are enriched in heavier Tl isotopes (Schauble 2007; Yang and Liu 2015). It has been proved that the traditional mass-dependent takes up about 25% of the total equilibrium fractionation at room temperature (Fujii et al. 2013).

The NVE is also known as the nuclear field shift (NFS). It is produced by the deviation of the nuclear field with different nuclear size for isotopes, which leads to the different electronic energy and density at the nuclei (Bigeleisen 1996; Schauble 2007). The NVE becomes larger as atomic mass increases. Heavy isotopes prefer to go into species with smaller electronic densities at the nucleus (Schauble 2007). Although previous studies have devoted to calculating the NVE-driven fractionations of Tl-bearing small species (Schauble 2007; Fujii et al. 2013; Yang and Liu 2015), none of these studies have calculated the NVE-driven fractionations for Tl-bearing crystalline materials (e.g., minerals). In this study, we calculated Tl isotope equilibrium fractionation factors for Tl-bearing ions, molecules, radicals and minerals under different temperatures. Our aim is to provide a foundation of equilibrium isotope fractionation studies of Tl isotope geochemistry and help people to explain observed Tl isotope signals in nature.

## 2 Methods

Equilibrium isotope fractionation for heavy elements (Pb, U, W, Tl, Os, etc.) contains the effect of mass shifts ( $\ln \alpha_0$ ) and the nuclear field shift (i.e., the nuclear volume effect) ( $\ln \alpha_{\text{NVE}}$ ) (Bigeleisen 1996). The mass-dependent fractionation scales with  $\delta m/m$ , and it declines with the decrease of the relative mass difference between different isotopes. When the atomic number is larger than 40, mass-dependent fractionation becomes very small even at ambient temperatures. Therefore, the NVE becomes the dominant factor of the total equilibrium isotope fractionation of heavy metal isotope systems (Pb, U, W, Tl, Os, etc.) (Bigeleisen 1996; Schauble 2007).

Based on the classical method suggested by Bigeleisen and Mayer (1947) and Urey (1947), the pure harmonic vibrational frequencies are required for the calculation of mass-dependent fractionation. Here, we follow the methods and procedures used in Schauble (2007) and Yang and Liu (2015) to calculate the mass-dependent part of Tl isotope fractionations. For gaseous molecules and ions containing  $\text{Tl}^+$  and  $\text{Tl}^{3+}$ , the Hartree–Fock (HF) method was applied in the Gaussian 09 software package (Frisch et al. 2009). The relativistic pseudopotential is used to consider the inner electronic potential energy, and we use the contraction double-zeta basis set cc-pVDZ-PP as the basis set for the outer electrons and the non-pseudopotential double-zeta basis set (cc-pVDZ) is chosen as the basis set for the light element (H, O, F, Cl, Br). Similarly, the results demonstrate that the contribution of mass-dependent fractionation is much smaller than that of NVE (Table 1).

**Table 1** Mass dependent fractionations ( $\epsilon_{205-203}^{\text{MD}} = 10,000 \cdot \rho_{205-203}^{\text{MD}}$ ) of Tl-bearing molecules relative to Tl atom, calculated in this study

substance	0 °C	25 °C	100 °C	300 °C	1000 °C	3000 °C
Tl	0.00	0.00	0.00	0.00	0.00	0.00
$\text{Tl}^+$	0.00	0.00	0.00	0.00	0.00	0.00
$\text{Tl}^{3+}$	0.00	0.00	0.00	0.00	0.00	0.00
TlF	2.20	1.88	1.24	0.54	0.11	0.02
$\text{TlF}_3$	9.37	8.03	5.34	2.37	0.49	0.08
TlCl	1.14	0.96	0.62	0.27	0.05	0.01
$\text{TlCl}_3$	5.93	5.02	3.25	1.40	0.29	0.04
TlBr	1.01	0.85	0.55	0.23	0.05	0.01
$\text{TlBr}_3$	5.25	4.43	2.85	1.22	0.25	0.04
$\text{Tl}_2\text{O}$	4.57	3.89	2.54	1.11	0.23	0.03
$\text{Tl}_2\text{S}$	2.30	1.94	1.25	0.53	0.11	0.02
$\text{Tl}(\text{H}_2\text{O})_3^+$	0.84	0.71	0.45	0.19	0.04	0.01
$\text{Tl}(\text{H}_2\text{O})_6^{3+}$	6.78	5.75	3.75	1.62	0.33	0.05

The nuclear field effect depends on the electronic density at the nucleus and the charge, shape, and size of the nucleus (Bigeleisen 1996). In this study, we only take into account the finite volume of the nucleus with spherical shapes of an atomic nucleus because the NVE dominates the nuclear field effect (Schauble 2013; Yang and Liu 2015, 2016). There are two quantum-chemistry-based methods that can be used to calculate the NVE-driven isotope fractionation. The first method is based on the change of ground-state electronic energy between two isotopologues. The fractionation factor can be expressed as (Bigeleisen 1996):

$$\ln \alpha_{\text{NVE}} = (kT)^{-1} \{ [E^0(\text{A}'\text{X}) - E^0(\text{AX})] - [E^0(\text{A}'\text{Y}) - E^0(\text{AY})] \} \quad (1)$$

where A and A' are light and heavy isotope of element A.  $E^0$  is the minimum of ground state electronic potential energy for two isotopologues AX and AY.

Several previous studies have used the Dirac–Hartree–Fock method to calculate the electronic energy of Tl-bearing species (Schauble 2007; Fujii et al. 2013; Yang and Liu 2015). Basis sets are set as four-component relativistic Gaussian basis sets for the heavy element. For open-shell systems, the complete open shell configuration (COSCI) method is considered. Three methods are accomplished with Dirac04, GRASP2 K and UTChem program respectively. There are small differences in the results of these methods (Table 2). Unfortunately, this ground-state energy calculation method can only be applied to systems with no more than 20 atoms (Schauble 2013), because the calculation of electronic energy in large systems is too computationally expensive and it is hard to obtain the required accuracy.

Another method, which can be applied into solid and liquid systems, is to obtain the NVE-driven fractionation factor from the electronic density at the nucleus. The difference of electronic energy between light- and heavy-isotope containing systems can be written as a relation of effective electronic density and the difference of mean-square nuclear charge radii (Almoukhalalati et al. 2016):

$$\delta E^{\text{AA}'} = E^0(\text{A}'\text{X}) - E^0(\text{AX}) = Z_{\text{A}} e^2 / 6\epsilon_0 \cdot \bar{\rho}_{\text{e}}^{\text{A}}(\text{AX}) \cdot \delta r_{\text{AA}'}^2 \quad (2)$$

where  $Z_{\text{A}}$  is atomic number of element A,  $e$  is an elementary charge ( $1.60217733 \times 10^{-19}$  C),  $\epsilon_0$  is permittivity of free space ( $8.854187817 \times 10^{-12}$  F/m),  $\delta r_{\text{AA}'}^2$  is the difference of mean-squared nuclear radii between  $^{205}\text{Tl}$  and  $^{203}\text{Tl}$  which can be obtained from (Angeli and Marinova 2013), and  $\bar{\rho}_{\text{e}}^{\text{A}}$  is the effective electronic densities at the nucleus of A in the target substance. Hence, we can

**Table 2** The comparison of NVE-driven fractionations (in  $\varepsilon^{205}\text{Tl}$ ) of Tl-bearing species relative to Tl atom at 298 K

		Schauble (2007) <sup>a</sup> Dirac04	Fujii et al. (2013) <sup>b</sup> GRASP2K	Fujii et al. (2013) <sup>c</sup> UTChem	Yang and Liu (2015) <sup>d</sup> Dirac04	This study ADF
Tl	Tl	0.00	0.00	0.00	0.00	0.00
Tl <sup>+</sup>	Tl <sup>+</sup>	− 2.20	− 2.21	− 1.57	− 2.30	− 1.78
	Tl(H <sub>2</sub> O) <sup>+</sup>			− 1.68		− 1.59
	TlCl			0.04		− 0.24
	TlO			2.83		2.17
	Tl(H <sub>2</sub> O) <sub>3</sub> <sup>+</sup>	− 1.10			− 1.90	− 1.46
Tl <sup>3+</sup>	Tl <sup>3+</sup>	25.50	25.68	25.01	25.40	21.45
	Tl(H <sub>2</sub> O) <sup>3+</sup>			18.98		12.28
	TlCl <sup>2+</sup>			− 6.77		5.22
	TlO <sup>+</sup>			− 0.18		− 1.78
	Tl(H <sub>2</sub> O) <sub>6</sub> <sup>3+</sup>	19.70			19.50	12.31

<sup>a</sup>Results are implemented by Dirac04 from Schauble (2007)

<sup>b</sup>Results are implemented by package GRASP2K from Fujii et al. (2013)

<sup>c</sup>Results are implemented by UTChem program from Fujii et al. (2013)

<sup>d</sup>Results are implemented by Dirac04 from Yang and Liu (2015)

deduce another formula from Eqs. (1) and (2) written as  $\ln K_{fs}$ :

$$\ln \alpha_{\text{NVE}} = (kT)^{-1} \left\{ Z_A e^2 / 6\epsilon_0 [\bar{\rho}_c^A(\text{AX}) - \bar{\rho}_c^A(\text{AY})] \delta r_{AA'}^2 \right\} \quad (3)$$

High-precision NVE calculations for solid systems need precise effective electronic densities based on the second method, but it is hard to achieve. The effective electronic density at the nucleus can typically be approximated by the so-called “contact electronic density”, which may lead to  $\sim 10\%$  errors (Almoukhalalati et al. 2016). The reason is that the contact density is the electronic density at the origin  $r = 0$  position of atom nucleus (Mastalerz et al. 2010), while the effective density represents electronic density at a radius inside the nuclear volume from 0 to R. We can obtain the average density of points on a small sphere around the center of a nucleus in ADF code, which can be a good approximation of the effective electronic energy and is a better treatment compared to that of the contact density.

There is only one previous study of NVE calculation for crystalline systems, and its focus was on Hg, Cd and Sn isotope systems (Schauble 2013). That study used the projector augmented wave (PAW) method implemented in ABINIT code and considered scalar relativistic treatment and Gaussian finite nuclear module to calculate the contact density at the nucleus for crystalline systems.

In this study, instead of calculating the contact density, we directly calculated the effective electronic density at the nucleus for both molecules and crystalline systems by using ADF software and BAND module built in it (Velde and Baerends 1991; Guerra et al. 1998; Velde et al. 2001).

ADF provides the basis sets of Slater-type for all elements. It is well-known that Slater-type basis sets can be more accurate to calculate nuclear cusp and long-range behaviors than Gaussian-type basis sets.

When the properties of heavy elements are calculated, it is reasonable to use the zeroth-order regular approximated (ZORA) relativistic approach and a Gaussian finite nucleus module. For gaseous molecules and ions, we used QZ4P (quadruple zeta with four polarization functions) ZORA basis sets to obtain very accurate results. For solid systems, TZ2P (triple zeta with two polarization functions) was selected, which helps to save calculation time and gets accurate results at the same time. We used the GGA-PBE functional with DFT approach to calculating electronic density at the nucleus in this study. When managing the aqueous species in water, we used the COSMO (Conductor-like Screening Model) solvation model to account for the solvation effects. As a result, the fractionation factors driven-by NVE can be obtained from Eq. (3) using the results of electronic densities at the nucleus. The comparison of the results of fractionation factors calculated in this study and the results from previous studies for Tl-bearing ions, molecules and radicals are shown in Table 2. The reason for the differences of final results is that the type of basis sets we used in this study is Slater-type, while other studies used Gaussian-type orbitals.

### 3 Results

The  $\varepsilon$  notation is commonly used for Tl isotope composition for natural samples:

$$\varepsilon^{205}\text{Tl} = \left( \frac{{}^{205}\text{Tl} / {}^{203}\text{Tl}}{\text{sample}} / \left( \frac{{}^{205}\text{Tl} / {}^{203}\text{Tl}}{\text{standard}} - 1 \right) \right) \times 10^4 \quad (4)$$

Accordingly, the calculated NVE-driven Tl isotope fractionation is written as

$$\varepsilon_{\text{NVE}}^{205}\text{Tl} = 10,000 \times \ln(\alpha_{\text{NVE}}) \quad (5)$$

where  $\alpha_{\text{NVE}}$  is the isotope fractionation factor caused by the NVE. The mass-dependent Tl isotope fractionation is expressed as

$$\varepsilon_{\text{MD}}^{205}\text{Tl} = 10,000 \times \ln(\alpha_{\text{MD}}) \quad (6)$$

where  $\alpha_{\text{MD}}$  is the isotope fractionation factor caused by mass-dependent isotope effect, which usually is governed by the Bigeleisen-Mayer equation or the Urey model (Bigeleisen and Mayer 1947; Urey 1947).

### 3.1 Mass-dependent fractionations in Tl-bearing systems

First, we have known that the traditional mass-dependent fractionation is much less than the NVE-driven fractionation for Tl isotope system (Fujii et al. 2013). The mass-dependent (MD) fractionation factor is proportional to  $\delta m/m'$  and  $1/T^2$  ( $\ln \alpha_{\text{MD}} \propto \delta m/m' T^2$ ) and the NVE-driven fractionation factor is proportional to the difference of mean-square nuclear radii and  $1/T$  ( $\ln \alpha_{\text{NVE}} \propto \delta r^2/T$ ). The above two relationships indicate that the small relative mass difference between  ${}^{203}\text{Tl}$  and  ${}^{205}\text{Tl}$  causes a minor mass-dependent fractionation, while the NVE-driven fractionation becomes the dominant factor for the overall fractionation, especially at high temperatures (Schauble 2007) (Tables 1, 3).

### 3.2 NVE-driven fractionations for Tl-bearing ions, molecules and radicals

The magnitude of the NVE is controlled by the oxidation states, the coordination number of Tl and the electronegativity of adjacent atoms to Tl. Tl mainly maintains two oxidation states (Tl(I) and Tl(III)). The results of NVE-driven fractionation for Tl-bearing ions, molecules and radicals suggest that heavier isotope  ${}^{205}\text{Tl}$  will be enriched in oxidized states (i.e.,  $\text{Tl}^{3+}$ -bearing species) compared to reduced states ( $\text{Tl}^+$ -bearing species) (Table 3). This rule of thumb has been suggested by previous studies (Schauble 2007; Fujii et al. 2013; Yang and Liu 2015). The largest equilibrium Tl isotope fractionation between  $\text{Tl}^{3+}$  ions and  $\text{Tl}^+$  ions is 21.44 (in  $10^{-4}$ ) at 25 °C (see Table 3 and there is no classical MD fractionation between  $\text{Tl}^{3+}$  ions and  $\text{Tl}^+$  ions).

It has been known that a decrease in s-shell electrons, as well as an increase in p, d, f electrons, could lead to less electronic density at the nucleus. Tl-species with less electronic density tend to be enriched in heavier isotopes and consequently exhibit a larger  $\varepsilon^{205}\text{Tl}$  value. Conversely, a heavy element with larger electronic densities at the nucleus can have a deficit of  $\varepsilon^{205}\text{Tl}$  (Bigeleisen 1996; Schauble 2007). The electron configuration of the  $\text{Tl}^+$  ion is  $((\text{Xe})4f^{14}5d^{10}6s^2)$ , which has one p-shell electron less than that of Tl atom  $((\text{Xe})4f^{14}5d^{10}6s^26p^1)$ . Therefore,  $\text{Tl}^+$  ion has larger electronic densities and a negative value of  $\varepsilon^{205}\text{Tl}$  relative to Tl atom. The  $\text{Tl}^{3+}$  ion  $((\text{Xe})4f^{14}5d^{10})$  has two s-shell electrons less than  $\text{Tl}^+$  ion  $((\text{Xe})4f^{14}5d^{10}6s^2)$ , hence  $\text{Tl}^{3+}$  ion has a smaller electronic density than both  $\text{Tl}^+$  ion and Tl atom. Heavier Tl isotopes should be enriched in  $\text{Tl}^{3+}$  species and to produce a large positive value of  $\varepsilon^{205}\text{Tl}$  (if relative to Tl). When  $\text{Tl}^+$  ion is connected to an anion, such as  $\text{O}^{2-}$ ,  $\text{F}^-$ ,  $\text{Cl}^-$ , and  $\text{Br}^-$ , the outer s-shell electrons of  $\text{Tl}^+$  will be shared by that anion. It decreases the electronic density at the nucleus of Tl. Specifically, when bonded to Tl, the electronic density declines as this order:  $\text{Tl-O} > \text{Tl-F} > \text{Tl-Cl} > \text{Tl-Br}$ . Such bonding produces a higher  $\varepsilon^{205}\text{Tl}$  value than that of Tl (Fig. 1a). On the contrary, the sharing of d electrons in the outer layer will increase the electronic density at the nucleus and decrease the value of  $\varepsilon^{205}\text{Tl}$  for  $\text{Tl}^{3+}$ -bearing systems. Compared  $\text{Tl}^{3+}$  ion with  $\text{Tl}(\text{H}_2\text{O})^{3+}$ ,  $\text{Tl}(\text{H}_2\text{O})_3^{3+}$  and  $\text{Tl}(\text{H}_2\text{O})_6^{3+}$ , we can find that the results of fractionation factors are similar to each other, while the composition of  ${}^{205}\text{Tl}$  for  $\text{Tl}^{3+}$  ion shows a bit heavier than the aqueous phases (Fig. 1b). As for  $\text{Tl}^+$ -bearing species, most of the aqueous phases show larger values of  $\varepsilon^{205}\text{Tl}$  compared to  $\text{Tl}^+$  ion. These characteristics are shown in Table 3.

Tl generally exists as Tl(I) in nature, and Tl(III) only exists in the surface environment or under high oxidizing conditions. Tl exists as  $\text{Tl}^+$  ion or  $\text{TlCl}$  in seawater. It has been reported that  $\text{Tl}^+$  in the seawater can be oxidized to  $\text{Tl}^{3+}$  on the surface of manganese-oxide (birnessite) during the process of absorption. This absorption could lead to an enrichment of Tl content and also  ${}^{205}\text{Tl}$  (Bidoglio et al. 1993; Peacock and Moon 2012). Tl could enter in the vacancy of hexagonal birnessite and be oxidized to  $\text{Tl}^{3+}$  while  $\text{Mn}^{4+}$  would be reduced to  $\text{Mn}^{2+}$ . According to the structure of sorption Tl in hexagonal birnessite observed in the experiments (Peacock and Moon 2012), Tl is tetrahedral with O atoms in the vacancy position. Two kinds of spatial structure of hexagonal birnessite were constructed. They are Tl\_HxBir\_pH8\_2 h (Fig. 2a) and Tl\_HxBir\_pH8\_336 h (Fig. 2b) (Peacock and Moon 2012). They are C3 symmetric, and their bond length is the same as that of  $\text{Tl}_2\text{O}_3$ . Other types of manganese oxides, such as todorokite, triclinic birnessite, and ferrihydrite, do not show the deficit of  $\varepsilon^{205}\text{Tl}$  and the transformation of the



**Table 3** Nuclear volume fractionations ( $\epsilon_{205-203}^{NV} = 10,000 \cdot \beta_{205-203}^{NV}$ ) of Tl-bearing molecules relative to Tl atom, calculated in this study

Substance	e 0 °C	25 °C	100 °C	300 °C	1000 °C	3000 °C
Tl	0.00	0.00	0.00	0.00	0.00	0.00
Tl <sup>+</sup>	− 1.94	− 1.78	− 1.42	− 0.92	− 0.42	− 0.16
TlF	0.09	0.08	0.07	0.04	0.02	0.01
TlCl	− 0.26	− 0.24	− 0.19	− 0.12	− 0.06	− 0.02
TlBr	− 0.31	− 0.29	− 0.23	− 0.15	− 0.07	− 0.03
Tl <sub>2</sub> O	0.67	0.61	0.49	0.32	0.14	0.06
Tl <sub>2</sub> S	0.15	0.13	0.11	0.07	0.03	0.01
Tl <sub>3</sub> As	0.19	0.17	0.14	0.09	0.04	0.02
Tl(H <sub>2</sub> O) <sup>+</sup>	− 1.74	− 1.59	− 1.27	− 0.83	− 0.37	− 0.15
Tl(H <sub>2</sub> O) <sub>3</sub> <sup>+</sup>	− 1.59	− 1.46	− 1.16	− 0.76	− 0.34	− 0.13
Tl(H <sub>2</sub> O) <sub>6</sub> <sup>+</sup>	− 2.09	− 1.92	− 1.53	− 1.00	− 0.45	− 0.17
TlO <sup>−</sup>	2.37	2.17	1.74	1.13	0.51	0.20
Tl <sup>3+</sup>	23.40	21.44	17.13	11.15	5.02	1.95
TlF <sub>3</sub>	9.32	8.54	6.82	4.44	2.00	0.78
TlCl <sub>3</sub>	7.25	6.64	5.31	3.45	1.55	0.60
TlBr <sub>3</sub>	6.34	5.81	4.64	3.02	1.36	0.53
Tl(OH) <sub>3</sub>	7.71	7.06	5.64	3.67	1.65	0.64
Tl(H <sub>2</sub> O) <sub>3</sub> <sup>3+</sup>	13.39	12.27	9.80	6.38	2.87	1.12
Tl(H <sub>2</sub> O) <sub>3</sub> <sup>3+</sup>	4.22	3.86	3.09	2.01	0.90	0.35
Tl(H <sub>2</sub> O) <sub>6</sub> <sup>3+</sup>	13.43	12.31	9.83	6.40	2.88	1.12
TlO <sup>+</sup>	− 1.94	− 1.78	− 1.42	− 0.92	− 0.42	− 0.16
TlCl <sup>2+</sup>	5.70	5.22	4.17	2.72	1.22	0.48

oxidation state for Tl. Therefore, the content of hexagonal birnessite in ferromanganese sediments determined the total redox state of Tl, the content of Tl element and isotope composition of <sup>205</sup>Tl. It is not confirmed yet whether the apparent enrichment of <sup>205</sup>Tl in ferromanganese sediments could be explained by the NVE-driven fractionation during exchanging process of Tl species between birnessite and seawater. We use two types of tetrahedral structure of Tl<sup>3+</sup> in hexagonal birnessite (i.e., Tl\_HxBir\_pH8\_2 h and Tl\_HxBir\_pH8\_336 h) as suggested in a previous study (Peacock and Moon 2012) to represent the Tl-bearing birnessite, and use Tl<sup>+</sup> or TlCl in solution as the aqueous Tl<sup>+</sup> phase in seawater. The final fractionation results of such exchange reaction can reach to 9.57 ε-unit at 25 °C (Table 4). This calculation has used the COSMO solvent model method to account for possible solvation effects.

### 3.3 NVE-driven Tl isotope fractionations for crystalline compounds

As a lithophile element, Tl<sup>+</sup> ion can replace K<sup>+</sup> in micas and feldspar due to their similar ion radius (Rader et al. 2018). Tl element also displays chalcophile characteristic and tends to form a covalent bond in sulfides (Wood et al. 2008; Kiseeva and Wood 2013). Hence, the Tl<sup>+</sup> ion can replace Ag<sup>+</sup> or Pb<sup>2+</sup> in sulfides and sulfosalts (Rader et al. 2018). It has been reported that sulfides contain the larger

value of ε<sup>205</sup>Tl and in contrast, micas and feldspar show the smaller values from the observations of natural samples. In this study, we calculated NVE-driven fractionation factors of many Tl-bearing crystalline compounds and minerals, relative to Tl crystal (Fm3m) (Olsen et al. 1994) (Table 4). The structures of crystalline compounds have been shown in Fig. 3. The results of the calculated Tl isotope fractionations are consistent with the results from measurements, which show maximum values of ε<sup>205</sup>Tl in sulfides and the deficits of <sup>205</sup>Tl in feldspar, muscovite, phlogopite and orthoclase, etc. The largest fractionation between the coexisting phases with the same oxidation state (Tl<sup>+</sup>) can reach to 0.95 ε-unit at 300 °C.

## 4 Discussion

### 4.1 Possible Tl isotope fractionations during analysis procedures

The measurement method of thallium isotopes has been largely improved since the late 1990s by using multiple collectors inductively coupled plasma-mass (MC-ICPMS) (Rehkamper and Halliday 1999), which provides a high precision of 0.01–0.02% for the ratio of <sup>205</sup>Tl/<sup>203</sup>Tl compared with previous studies measured by NTIMS (Nielsen et al. 2017). They used the power law with a known ratio of

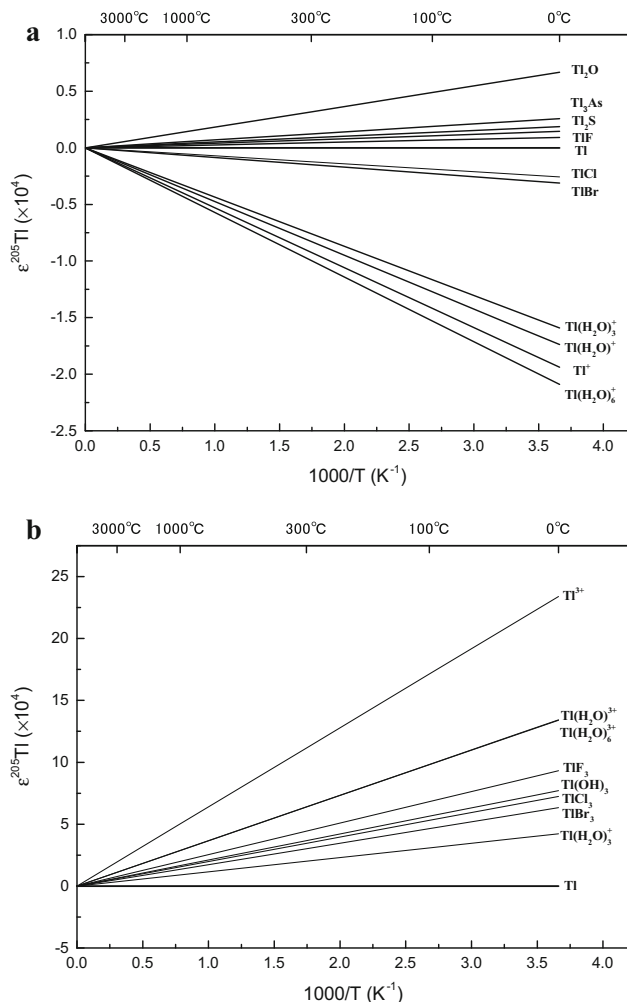


**Fig. 1** **a** Tl isotope fractionations driven by the nuclear volume effect for  $Tl^{+}$ -bearing ions and molecules relative to Tl atom; **b** Tl isotope fractionations driven by the nuclear volume effect for  $Tl^{3+}$ -bearing ions and molecules relative to Tl atom

$^{208}Pb/^{206}Pb$  in solution to correct the mass bias of  $^{205}Tl/^{203}Tl$ . This approach can help to clear the equilibrium and kinetic fractionations that are mass-dependent during the experiment (Rehkamper and Halliday 1999; Nielsen et al. 2004). However, there must be NVEs during the chemical treatment processes and mass spectrometric analysis.

Thallium mostly exists as  $Tl^{+}$  ion with a small amount of  $Tl^{3+}$  ion (0.2–0.5%) coexisting in measured solutions at ambient temperature environment (Fujii et al. 2013), and they form halide complexes with anions like  $F^{-}$ ,  $Cl^{-}$  and  $Br^{-}$  (Rehkamper and Halliday 1999; Fujii et al. 2013). It is essential to have all  $Tl^{+}$  ions are oxidized to  $Tl^{3+}$ , for  $Tl^{+}$  cannot form ion complexes strong enough to entirely enter anion exchange resins (Nielsen et al. 2011; Nielsen et al. 2017). Without full oxidation,  $Tl^{+}$  would be missing, conducting to Tl isotope fractionation (Nielsen et al. 2017).

As shown in Table 3, the NVE-driven fractionation between aqueous  $Tl^{3+}$  and aqueous  $Tl^{+}$  can reach to about 23  $\epsilon$ -unit at room temperature.

The difference of  $\epsilon^{205}Tl$  between aqueous  $TlCl_n^{3-n}$  and aqueous  $TlCl_n^{1-n}$  ( $n = 1, 2, 3, 4$ ) can be up to 7.8 at 25  $^{\circ}C$ . When the aqueous phase is ionized in the mass spectrometer, aqueous  $Tl^{3+}$  or  $TlCl_n^{3-n}$  will change into  $Tl^{+}$  ion. The NVE can cause about 20  $\epsilon$ -unit decline of  $\epsilon^{205}Tl$  at instrument operating temperature if the ionization process is incomplete.

Therefore, it should be noted that the NVE-driven fractionation in Tl isotope analysis would not be eliminated efficiently if the  $Tl^{+}$  could not be completely transformed into  $Tl^{3+}$ , or if  $Tl^{3+}$ -complexes could not be completely inhaled via ionization.

## 4.2 The NVEs in natural processes

The NVE can take place in the process of exchange, segregation and migration processes of Tl. Such natural processes as the exchange between seawater and sediments, thermal alteration, phase transition, fluid metasomatism and large impacts have been observed to result in Tl isotope fractionations (Palk et al. 2011). The variation of  $\epsilon^{205}Tl$  for terrestrial samples is larger than 35  $\epsilon$ -unit (Nielsen et al. 2017). For example, low temperature altered oceanic crust carries a deficit of  $^{205}Tl$  ( $-20 \epsilon$ ), and ferromanganese sediments carry an enrichment of  $^{205}Tl$  ( $+15 \epsilon$ ) in the marine environment (Rehkamper et al. 2002; Nielsen et al. 2006b, 2013). The redox potential of  $Tl^{+}$  to  $Tl^{3+}$  is  $-1.28$  V. The oxidation state Tl(III) only exists at highly oxidizing conditions for terrestrial samples (Nielsen et al. 2017). The positive anomalies of  $\epsilon^{205}Tl$  ( $+4 \sim +15$ ) are thought to be caused by the transformation of thallium's redox state during the exchange of Tl ion between hydrogenetic manganese oxide and seawater. This process is accompanied by NVE-driven fractionation (Peacock and Moon 2012; Nielsen et al. 2013). The adsorption simulation experiment found that  $Tl^{+}$  could be absorbed into the vacancy site of oxygen tetrahedron structure in hexagonal birnessite, and  $Tl^{+}$  could be oxidized to  $Tl^{3+}$  at the same time (Peacock and Moon 2012). It has been discussed that the variation of  $\epsilon^{205}Tl$  between manganese oxide and seawater is dominated by NVE (Rehkamper et al. 2002; Koschinsky and Hein 2003; Schauble 2007; Nielsen et al. 2017). In this study, we have used two structures of hexagonal birnessite with  $Tl^{3+}$  added in the vacancy (Fig. 2), and calculated their fractionation factors driven by NVE relative to  $Tl^{+}$  species in seawater ( $Tl^{+}(aq)$  and  $TlCl(aq)$ ) (Peacock and Moon 2012). In our simulation, we considered simulating the process of exchanging and oxidizing  $Tl^{+}$  between seawater and manganese oxide as a long-time and equilibrium

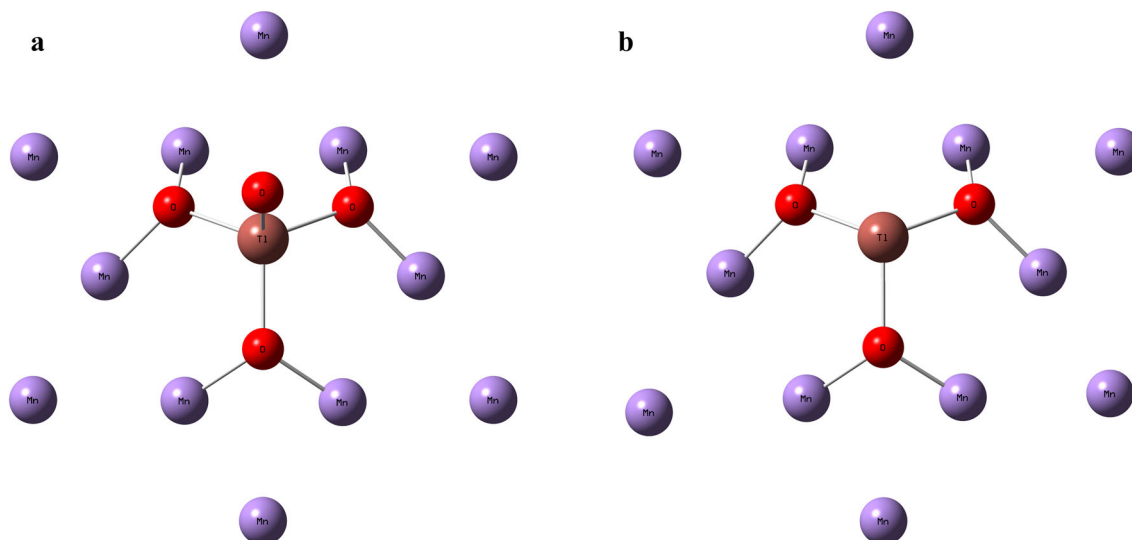


**Fig. 2** **a** The structure of Tl\_HxBir\_pH8\_2h; **b** The structure of Tl\_HxBir\_pH8\_336h (Peacock and Moon 2012)

**Table 4** NVE-driven fractionations ( $\epsilon_{205-203}^{NV} = 10,000 \cdot \beta_{205-203}^{NV}$ ) between two types of hexagonal birnessite and species in seawater

	0 °C	25 °C	100 °C	300 °C
Tl_HxBir_pH8_2h(aq)-Tl <sup>+</sup> (aq)	10.45	9.57	7.65	4.98
Tl_HxBir_pH8_2h(aq)-TlCl(aq)	9.97	9.13	7.30	4.75
Tl_HxBir_pH8_336h(aq)-Tl <sup>+</sup> (aq)	8.39	7.69	6.14	4.00
Tl_HxBir_pH8_336h(aq)-TlCl(aq)	7.91	7.25	5.79	3.77

process. As shown in Table 4,  $^{205}\text{Tl}$  tends to be enriched in hexagonal birnessite relative to  $\text{Tl}^+$  species in seawater, and the NVE-driven fractionation can reach to  $9.57 \epsilon^{205}\text{Tl}$  at 25 °C. This value provides a reasonable explanation for the positive anomalies found in ferromanganese sediments (Table 5).

In addition, during the condensation process of the early solar system, Tl could exist in the form of diverse valence states at the high-T solar nebula. Total fractionation among Tl-bearing species was probably dominated by NVE when fractionation process reached equilibrium. According to the data in Fig. 4, the fractionation driven by NVE of  $\text{Tl}_2\text{O}$  relative to Tl atom is  $0.21 \epsilon^{205}\text{Tl}$  and the fractionation of  $\text{Tl}_2\text{S}$  relative to Tl atom is  $0.05 \epsilon^{205}\text{Tl}$  at 600 °C. The maximum value of the fractionation reaches to  $7.93 \epsilon^{205}\text{Tl}$  between  $\text{Tl}^+$  ion and  $\text{Tl}^{3+}$  ion at 600 °C. As we can see that NVE-driven fractionation is not prominent among gas species at high-T. Also, if the process reached to phase equilibrium during the early stage of evaporation and condensation, the NVE-driven fractionation between two phases, such as  $\text{Tl}_2\text{S}(\text{g})$  to  $\text{Tl}_2\text{S}(\text{s})$  can reach  $-0.49 \epsilon^{205}\text{Tl}$  at the condensation temperature of Tl (532 K). Therefore, only the NVE-driven fractionation cannot explain a 50- $\epsilon$  fractionation among meteorite samples, ranging from  $-20$  to  $+30 \epsilon^{205}\text{Tl}$  (Nielsen et al. 2006a; Andreasen et al. 2009; Palk et al. 2011; Nielsen et al. 2017). The uneven

distribution of Tl isotopes in meteorite samples was resulted from the combination of stable isotope fractionation and the decay of the  $^{205}\text{Pb}$  isotope. It is generally believed that the evaporation and condensation process in the early solar system is controlled by the process of kinetic isotope fractionation (Nielsen et al. 2017).

The abundance of Tl in CI chondrites is much higher than that in the mantle (0.14 ppm in CI vs. 0.0041 ppm in the mantle) (Palme 2014), which indicates that Tl is most likely to have evaporated into space or to have entered the core during the accretion of Earth. It has been known that Tl has an affinity with sulfur and Tl tended to enter the core along with sulfur during the process of core formation, according to the high Tl content of the sulfide (Coggon et al. 2009). This process would result in the Tl differentiation and isotope fractionation between mantle and core. Moreover, it has been measured that the partition coefficient of Tl in sulfide fluid/silicate melt equals to 4.1–18.8 (Kiseeva and Wood 2013), indicating that sulfide is indeed the primary carrier of Tl in the mantle. Therefore, Tl is readily to be carried away by sulfide fluid and transported by magmatic fluid in the hydrothermal and partial melting processes (Nielsen et al. 2014). If Tl in mineral were partially removed as  $\text{Tl}_2\text{S}$  by sulfide fluid, the equilibrium fractionation driven by NVE could reach  $-4.83$  to  $+1.86 \epsilon^{205}\text{Tl}$  at 300 °C, minerals including sulfides and silicates



**Fig. 3** The structures of Tl-bearing crystalline compounds used for the calculation: Tl (Fm3m) (Olsen et al. 1994); Tl (Im3m) (Schneider and Heymer 1956); Tl<sub>2</sub>S(R3) (Mullen and Nowacki 1972); TlF(Fm3m) (Ketelaar 1935); TlCl(Fm3m) (Moeller 1933); Galena (Noda et al. 1987); Djerfisherite (Zaccarini et al. 2007); Orpiment (Mullen and Nowacki 1972); Sphalerite (Nitta et al. 2008); Chalcopyrite (Knight et al. 2011); Muscovite (Richardson and Richardson 1982); Phlogopite (Hendricks and Jefferson 1939); Feldspar (Taylor 1934); Astrophyllite (Piilonen et al. 2003); Jarosite (Basciano and Peterson 2007)

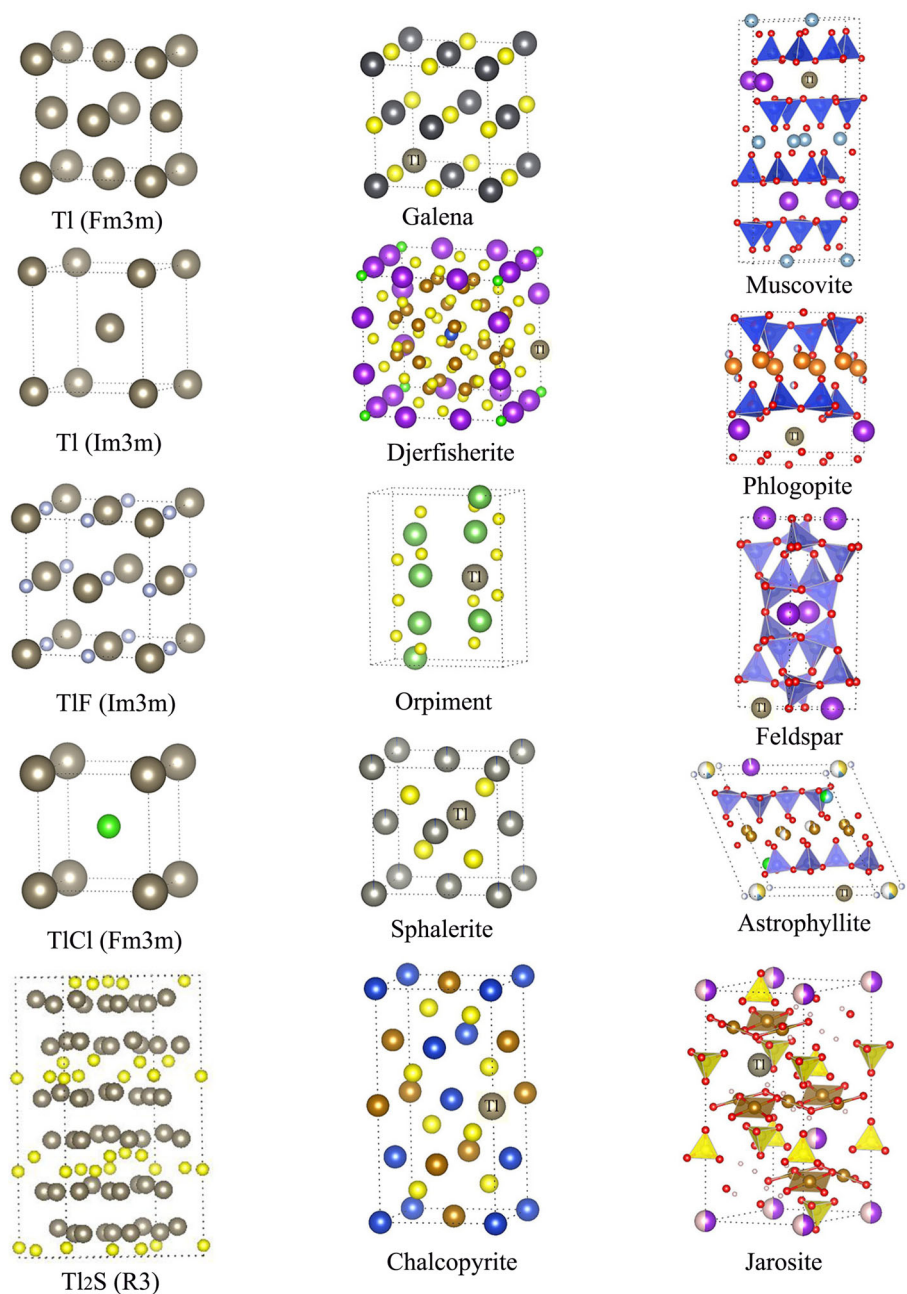


(Fig. 4). In the process of magmatic segregation, the fractionation of co-existing phases, silicate/sulfide is up to  $1.96 \epsilon^{205}\text{Tl}$  (chalcopyrite/muscovite) at  $1000 \text{ }^\circ\text{C}$  (Fig. 4). When measuring the natural minerals,  $^{205}\text{Tl}$  was found to be enriched in sulfides. The silicate minerals, like micas and feldspar, have a deficit of  $^{205}\text{Tl}$  (Rader et al. 2018). In experiments on the differentiation between sulfides and silicates, the fractionation of the co-existing phases can reach  $+0.2$  to  $+0.3 \epsilon^{205}\text{Tl}$  at  $1650 \text{ }^\circ\text{C}$  (Wood et al. 2008). We have calculated the NVE fractionations between Tl-bearing crystals, sulfides, sulfosalts, silicates, and Tl (Fm3m) (Fig. 4). The isotope fractionations driven by NVE

of  $^{205}\text{Tl}/^{203}\text{Tl}$  range from 0.17 to 0.38 at  $1650 \text{ }^\circ\text{C}$  between sulfides and silicates, which is consistent with the experimental data.

### 4.3 The Tl isotope constraint on Earth's late veneer

Late veneer is a late accretion process which occurred after the core segregation. The contents of highly siderophile elements (HSEs) of the mantle were used to estimate how much material was delivered during the late veneer period (Day et al. 2007; Walker 2014).

**Table 5** NVE-driven fractionations ( $\epsilon_{205-203}^{NV} = 10,000 \cdot \beta_{205-203}^{NV}$ ) of Tl-bearing minerals relative to Tl (Fm3m), calculated in this study

substance	0 °C	25 °C	100 °C	300 °C	1000 °C	2000 °C
Tl (Fm3m)	0.00	0.00	0.00	0.00	0.00	0.00
Tl (Im3m)	- 1.19	- 1.09	- 0.87	- 0.56	- 0.25	- 0.14
Tl <sub>2</sub> S	- 1.88	- 1.72	- 1.38	- 0.90	- 0.40	- 0.23
Tl <sub>2</sub> O	- 0.87	- 0.79	- 0.64	- 0.41	- 0.19	- 0.10
TlF (Fm3m)	- 3.05	- 2.79	- 2.23	- 1.45	- 0.65	- 0.37
TlCl (Fm3m)	- 2.96	- 2.71	- 2.16	- 1.41	- 0.63	- 0.36
Galena	1.04	0.96	0.76	0.50	0.22	0.13
Djerfisherite	- 2.75	- 2.52	- 2.01	- 1.31	- 0.59	- 0.33
Orpiment	4.93	4.52	3.61	2.35	1.06	0.59
Sphalerite	2.59	2.37	1.89	1.23	0.56	0.31
Chalcopyrite	5.27	4.83	3.86	2.51	1.13	0.63
Muscovite	- 3.88	- 3.56	- 2.84	- 1.85	- 0.83	- 0.47
Phlogopite	- 3.39	- 3.10	- 2.48	- 1.61	- 0.73	- 0.41
Feldspar	- 3.20	- 2.93	- 2.34	- 1.53	- 0.69	- 0.38
Orthoclase	- 1.56	- 1.43	- 1.14	- 0.74	- 0.33	- 0.19
Astrophyllite	- 3.07	- 2.82	- 2.25	- 1.46	- 0.66	- 0.37
Jarosite	- 2.73	- 2.50	- 2.00	- 1.30	- 0.59	- 0.33

The structures of minerals and crystals are taken from following references: Tl (Fm3m) (Olsen et al. 1994); Tl (Im3m) (Schneider and Heymer 1956); Tl<sub>2</sub>S(R3) (Mullen and Nowacki 1972); Tl<sub>2</sub>O(R3m) (Sabrowsky 1971); TlF(Fm3m) (Ketelaar 1935); TlCl(Fm3m) (Moeller 1933); Galena (Noda et al. 1987); Djerfisherite (Zaccarini et al. 2007); Orpiment (Mullen and Nowacki 1972); Sphalerite (Nitta et al. 2008); Chalcopyrite (Knight et al. 2011); Muscovite (Richardson and Richardson 1982); Phlogopite (Hendricks and Jefferson 1939); Feldspar (Taylor 1934); Orthoclase (Viswanathan and Kielhorn 1983); Astrophyllite (Piilonen et al. 2003); Jarosite (Basciano and Peterson 2007)

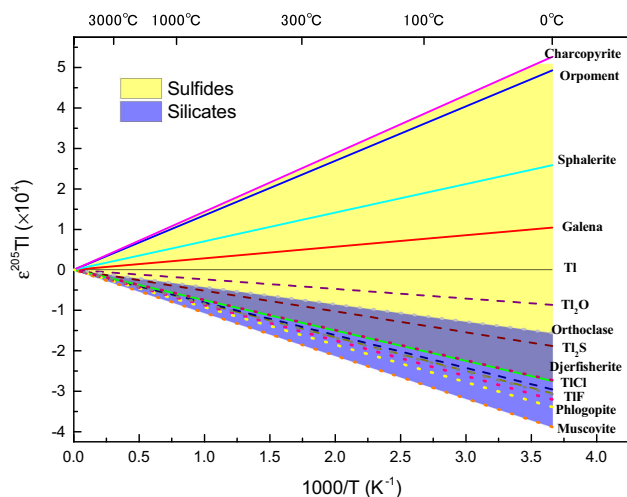


**Fig. 4** Tl isotope fractionations driven by the nuclear volume effect for Tl-bearing crystalline compounds relative to Tl (Fm3m). The yellow area represents the results for sulfide minerals and the blue area represents the results for silicate minerals

By using the average Tl concentration of 500 ng/g for the continental crust, 200 ng/g for the oceanic crust and 0.7 ng/g for the mantle, the content of Tl in bulk silicate Earth (BSE) has been estimated to be about 3.03 ng/g (Shaw 1952; McDonough and Sun 1995; Salters and Stracke 2004; Nielsen et al. 2006c, 2014). If we assume

that Tl would not enter the core during the process of core formation, which is based on the fact that the abundance of Tl is generally less than 0.02 ng/g in magmatic iron meteorites (Andreasen et al. 2012). We can also assume that the pristine mantle would be volatile-free after the accretion of proto-Earth, because of the highly volatile characteristic of Tl and the very low Tl concentration of current BSE relative to the chondrites and the similar Tl isotope composition between BSE and chondrites (Baker et al. 2010; Palk et al. 2018). Therefore, the very low content of Tl in the current BSE was almost entirely delivered by the late veneer.

In this case, considering the similar contents of Tl of enstatite chondrites (EC) and carbonaceous chondrites (CC) (Baker et al. 2010; Palk et al. 2011, 2018) (Fig. 5), we use an average value (50 ng/g) to represent EC and CC. Meanwhile, the average concentration of Tl in ordinary chondrites (OC) is 6 ng/g (Andreasen et al. 2009). We set  $x$  as the fraction of material from CC and EC delivered in the late veneer stage relative to the total mass of the Earth, and the fraction of OC is  $y$ . Previous HSEs estimate have suggested that the total value of late-stage substances accounts for 0.3–0.8 wt% of the total mass of the Earth (0.5 wt% on average). In that case,  $x + y = 0.5\%$ . If we assume that the material of late-stage accretion had constituted the entire Tl of BSE (the concentration of Tl in

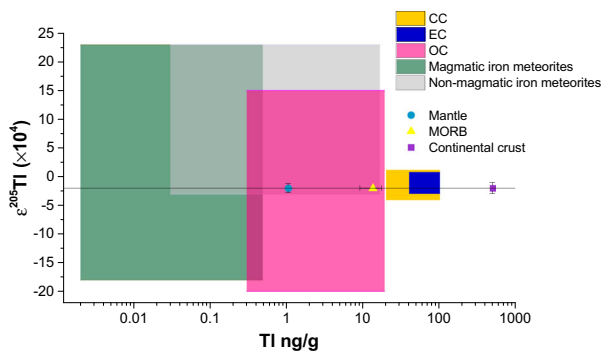


**Fig. 5** The content of Tl and the Tl isotope compositions of the Earth and meteorite samples (Palk et al. 2011; Baker et al. 2010; Andreassen et al. 2009; Nielsen et al. 2006a)

BSE is defined as  $n_{\text{BSE}}$  (ng/g), then,  $50x + 6y = n_{\text{BSE}}$  and  $n_{\text{BSE}} = 3.03 \times 67.4\% = 2.04$  (ng/g), which is the observed value for BSE. If  $0 \leq x \leq 0.5\%$ , because  $n_{\text{BSE}} = 44x + 3\%$ , then we get  $0.03 \leq n_{\text{BSE}} \leq 0.25$  ng/g, which is much smaller than the observed value of BSE, i.e., 2.04 ng/g (Fig. 6). The maximum value is only about one-tenth of the observed BSE value. It means it needs more chondritic materials, especially CC and EC. When  $x$  is larger than 4.0%,  $n_{\text{BSE}}$  can be larger than 2.04 ng/g. The value can be close to the observed value 2.04 (Fig. 6). Therefore, the amount of 0.5 wt% late veneer is not enough to explain the Tl content in BSE. It needs at least 5 times of materials estimated by HSEs [i.e.,  $5 \times (0.3 - 0.8 \text{ wt}\%) = (1.5 - 4.0 \text{ wt}\%)$ ].

Due to the high volatility of Tl, most of Tl was dissipated during the early Earth evaporation (McDonough 2014), and kinetic fractionation caused heavy Tl isotope to be left behind. The fractionation factor can be expressed as  $\alpha$ , and  $\alpha = (M_1/M_2)^\beta$ , where  $\beta = 0.5$  under vacuum. When the volatile species was  $\text{Tl}_2\text{S}$ , then  $\alpha = 1.0022$ , which would result in a 22- $\epsilon$  fractionation. However, such large

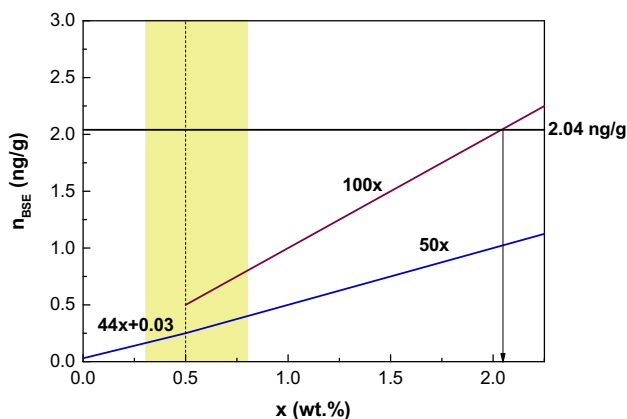


**Fig. 6** The relation between the fraction of late-accreted mass of enstatite chondrites and carbonaceous chondrites ( $x$ ) and the entire Tl concentration of BSE ( $n_{\text{BSE}}$ )

fractionation has not been found between BSE and undifferentiated chondrites. On the contrary, Tl isotope composition of BSE is slightly lighter instead of becoming heavier. Considering the condensation temperature of  $\text{Tl}_2\text{S}$  is only 523 K, it probably means that Tl could be completely evaporated during the early Earth, no matter it is in silicates or in sulfides.

Supposing that all of the Tl content in BSE came from the late veneer, it would be necessary for more chondrites to be added to the proto-Earth. We used the most massive abundance of CI chondrite as the upper limit of the Tl content (100 ng/g) (Baker et al. 2010). Then, the proportion of late veneer defined as  $k_{\text{LV}}$  could be obtained from the following formula:  $100 \times k_{\text{LV}} = n_{\text{BSE}}$  and  $n_{\text{BSE}} = 2.04$ . Finally,  $k_{\text{LV}}$  equals to 2.04% which is about five times larger than 0.5% (Fig. 6). This result is consistent with the magnitude of late veneer suggested by the new SPH simulation (Marchi et al. 2018) and the oxygen isotopic evidence (Greenwood et al. 2018).

The Tl isotope composition in the BSE is slightly lighter than that in CC and EC (Fig. 5). As shown in Fig. 4, there is a about 2  $\epsilon$ -unit fractionation of  $^{205}\text{Tl}/^{203}\text{Tl}$  between the sulfides and the silicates at high temperature (1000 °C). Tl would be carried away as the sulfide in the mantle, leaving a lighter part into the silicate phase. This indeed suggests that there were sulfides occurred during the last stage of core segregation. The sulfides could be transferred and entered the core or at somewhere in the mantle that haven't been found right now. Wood et al. (2008) believed that the metal phase would take away 50% of Tl from the BSE into the core. This process could lead to a deficit of  $^{205}\text{Tl}/^{203}\text{Tl}$  in silicate phase in modern BSE, which is about  $-2 \epsilon^{205}\text{Tl}$ . If this is the case, there must be much more materials to be delivered to Earth than what previously estimated.

## 5 Conclusions

In this study, an improved method was used for the first time to calculate the Tl isotope fractionation factors driven by the nuclear volume effect for Tl-bearing species, including ions, molecules, radicals, aqueous species and crystalline minerals. The improved method uses direct calculation of the effective electronic density instead of the contact electronic density. We found that oxidized  $\text{Tl}^{3+}$ -bearing species are more enriched in heavier Tl isotopes than  $\text{Tl}^+$ -bearing species. The maximum fractionation is 23.21  $\epsilon^{205}\text{Tl}$  at 25 °C between  $\text{Tl}^{3+}$  ion and  $\text{Tl}^+$  ion. The fractionation between hexagonal birnessite with Tl in the vacancy and  $\text{Tl}^+$  species in the seawater reaches 9.57  $\epsilon^{205}\text{Tl}$  at ambient temperature. This fractionation value can adequately explain the enrichment of  $^{205}\text{Tl}$  observed in the ferromanganese sediments. We find that Tl-bearing sulfides

concentrate  $^{205}\text{Tl}$  relative to silicates, and the variation ranging from 0.17 to 0.38  $\epsilon$ -unit at 1650 °C agrees with the results from the experiment of sulfide/silicate segregation. The change of redox state of Tl during the experiment can also lead to 20  $\epsilon$ -unit fractionation that is crucial in the study of Tl isotope fractionations. In conclusion, the nuclear volume effect of Tl isotopes plays an essential role in both natural and experimental processes, and our theoretical calculation provides a foundation for explaining the variations of  $\epsilon^{205}\text{Tl}$  in nature.

The Tl content and Tl isotope composition of BSE provides a constraint on the late veneer of Earth. We found that, based on the Tl content and its isotopic signal of BSE, the amount of materials delivered in the late veneer is more than five times than that estimated from HSEs. We also found that there is a sulfide-phase that occurred during the last stage of core segregation and may take away part of Tl to the core or deep mantle.

**Acknowledgements** All the calculations have been done on TianHe-2 supercomputer. Dr. Y.L. appreciates the funding supports from the strategic priority research program (B) of CAS (XDB18010100) and Chinese NSF projects (Nos. 41530210, 41490635).

## References

- Almoukhalalati A, Shee A, Saue T (2016) Nuclear size effects in vibrational spectra. *Phys Chem Chem Phys* 18:15406–15417
- Andreassen R, Schonbachler M, Rehkamper M (2009) The Pb-205-(Tl)-205 and Cd isotope systematics of ordinary chondrites. *Geochim Cosmochim Acta* 73:A43–A43
- Andreassen RRM, Benedix GK, Theis KJ, Schönbachler M, Smith CL (2012) Lead-thallium chronology of IIAB and IIIAB iron meteorites and the solar system initial abundance of lead-205. In: 43rd Lunar and planetary science conference, p 1659
- Angeli I, Marinova KP (2013) Table of experimental nuclear ground state charge radii: an update. *At Data Nucl Data Tables* 99:69–95
- Baker RGA, Schonbachler M, Rehkamper M, Williams HM, Halliday AN (2010) The thallium isotope composition of carbonaceous chondrites—new evidence for live Pb-205 in the early solar system. *Earth Planet Sci Lett* 291:39–47
- Basciano LC, Peterson RC (2007) Jarosite–hydronium jarosite solid solution series with full iron occupancy: mineralogy and crystal chemistry. *Am Miner* 92:1464–1473
- Bidoglio G, Gibson PN, Ogorman M, Roberts KJ (1993) X-ray-absorption spectroscopy investigation of surface redox transformations of thallium and chromium on colloidal mineral oxides. *Geochim Cosmochim Acta* 57:2389–2394
- Bigeleisen J (1996) Nuclear size and shape effects in chemical reactions. *Isotope chemistry of the heavy elements*. *J Am Chem Soc* 118:3676–3680
- Bigeleisen J, Mayer MG (1947) Calculation of equilibrium constants for isotopic exchange reactions. *J Chem Phys* 15:261–267
- Coggon RM, Rehkamper M, Atteck C, Teagle DAH (2009) Constraints on hydrothermal fluid fluxes from Tl geochemistry. *Geochim Cosmochim Acta* 73:A234–A234
- Day JMD, Pearson DG, Taylor LA (2007) Highly siderophile element constraints on accretion and differentiation of the Earth–Moon system. *Science* 315:217–219
- Frisch MJ et al (2009) Gaussian software package, Inc., Wallingford CT. Gaussian09, Revision D.01
- Fujii T, Moynier F, Agranier A, Ponzevera E, Abe M, Uehara A, Yamana H (2013) Nuclear field shift effect in isotope fractionation of thallium. *J Radioanal Nucl Chem* 296:261–265
- Greenwood RC et al (2018) Oxygen isotopic evidence for accretion of Earth's water before a high-energy Moon forming giant impact. *Sci Adv* 4:eao5928
- Guerra C, Snijders JG, Velde G, Baerends EJ (1998) Towards an order-N DFT method. *Theor Chem Acc* 99:391
- Heinrichs H, Schulzdobrick B, Wedepohl KH (1980) Terrestrial geochemistry of Cd, Bi, Tl, Pb, Zn and Rb. *Geochim Cosmochim Acta* 44:1519–1533
- Hendricks SB, Jefferson ME (1939) Polymorphism of the micas with optical measurements. *Am Miner* 24:729–771
- Hettmann K et al (2014) The geochemistry of Tl and its isotopes during magmatic and hydrothermal processes: the peralkaline Ilimaussaq complex, southwest Greenland. *Chem Geol* 366:1–13
- Ketelaar J (1935) Die Kristallstruktur des Thallofluorids. *Z Kristallogr Kristallgeom Kristallphys Kristallchem* 92:30–38
- Kiseeva ES, Wood BJ (2013) A simple model for chalcophile element partitioning between sulphide and silicate liquids with geochemical applications. *Earth Planet Sci Lett* 383:68–81
- Knight K, Marshall W, Zochowski S (2011) The low-temperature and high-pressure thermoelastic and structural properties of chalcopyrite,  $\text{CuFeS}_2$ . *Can Miner* 49:1015–1034
- Koschinsky A, Hein JR (2003) Uptake of elements from seawater by ferromanganese crusts: solid-phase associations and seawater speciation. *Mar Geol* 198:331–351
- Lodders K (2003) Solar system abundances and condensation temperatures of the elements. *Astrophys J* 591:1220–1247
- Marchi S, Canup RM, Walker RJ (2018) Heterogeneous delivery of silicate and metal to the Earth by large planetesimals. *Nat Geosci* 11:77–84
- Mastalerz R, Widmark PO, Roos BO, Lindh R, Reiher M (2010) Basis set representation of the electron density at an atomic nucleus. *J Chem Phys* 133(14):144111. <https://doi.org/10.1063/1.3491239>
- McDonough WF (2014) Treatise on geochemistry (second edition). 3.16-Compositional model for the Earth's core reference module in Earth systems and environmental sciences, vol 3, pp 559–577
- McDonough WF, Sun SS (1995) The composition of the Earth. *Chem Geol* 120:223–253
- McGoldrick PJ, Keays RR, Scott BB (1979) Thallium—sensitive indicator of rock-seawater interaction and of sulfur saturation of silicate melts. *Geochim Cosmochim Acta* 43:1303–1311
- Moeller K (1933) Eine fuer Praezisionsbestimmungen von Gitterkonstanten nach der Debye-Scherrer-Methode besonders geeignete Eichsubstanz. *Naturwissenschaften* 21:223
- Moynier F, Fujii T, Brennecka GA, Nielsen SG (2013) Nuclear field shift in natural environments. *C R Geosci* 345:150–159
- Mullen D, Nowacki W (1972) Refinement of the crystal structures of realgar,  $\text{AsS}$  and orpiment,  $\text{As}_2\text{S}_3$ . *Zeitschrift fur Kristallographie* 136:48–65
- Nielsen SG (2011) Thallium isotopes and their application to problems in earth and environmental science. In: Baskaran M (ed) *Handbook of environmental isotope geochemistry*. Springer, Berlin
- Nielsen SG, Rehkamper M, Baker J, Halliday AN (2004) The precise and accurate determination of thallium isotope compositions and concentrations for water samples by MC-ICPMS. *Chem Geol* 204:109–124



- Nielsen SG et al (2005) Thallium isotope composition of the upper continental crust and rivers—an investigation of the continental sources of dissolved marine thallium. *Geochim Cosmochim Acta* 69:2007–2019
- Nielsen SG, Rehkamper M, Halliday AN (2006a) Large thallium isotopic variations in iron meteorites and evidence for lead-205 in the early solar system. *Geochim Cosmochim Acta* 70:2643–2657
- Nielsen SG, Rehkamper M, Norman MD, Halliday AN, Harrison D (2006b) Thallium isotopic evidence for ferromanganese sediments in the mantle source of Hawaiian basalts. *Nature* 439:314–317
- Nielsen SG, Rehkamper M, Teagle DAH, Butterfield DA, Alt JC, Halliday AN (2006c) Hydrothermal fluid fluxes calculated from the isotopic mass balance of thallium in the ocean crust. *Earth Planet Sci Lett* 251:120–133
- Nielsen SG, Rehkamper M, Brandon AD, Norman MD, Turner S, O'Reilly SY (2007) Thallium isotopes in Iceland and Azores lavas—implications for the role of altered crust and mantle geochemistry. *Earth Planet Sci Lett* 264:332–345
- Nielsen SG, Wasylenko LE, Rehkamper M, Peacock CL, Xue ZC, Moon EM (2013) Towards an understanding of thallium isotope fractionation during adsorption to manganese oxides. *Geochim Cosmochim Acta* 117:252–265
- Nielsen SG, Shimizu N, Lee CTA, Behn MD (2014) Chalcophile behavior of thallium during MORB melting and implications for the sulfur content of the mantle. *Geochem Geophys Geosyst* 15:4905–4919
- Nielsen SG, Klein F, Kading T, Blusztajn J, Wickham K (2015) Thallium as a tracer of fluid–rock interaction in the shallow Mariana forearc. *Earth Planet Sci Lett* 430:416–426
- Nielsen SG, Rehkamper M, Prytulak J (2017) Investigation and application of thallium isotope fractionation. *Rev Miner Geochem* 82:759–798
- Nitta E et al (2008) Crystal chemistry of ZnS minerals formed as high-temperature volcanic sublimates: matraite identical with sphalerite. *J Miner Pet Sci* 103:145–151
- Noda Y, Masumoto K, Ohba S, Saito Y, Toriumi K, Iwata Y, Shibuya I (1987) Temperature dependence of atomic thermal parameters of lead chalcogenides, PbS, PbSe and PbTe Locality: synthetic Sample:  $t = 120$  K. *Acta Crystallogr Sect C* 43:1443–1445
- Olsen JS, Steenstrup S, Geward L, Johnson E (1994) A high-pressure study of thallium. *J Appl Crystallogr* 27:1002–1005
- Palk CS, Rehkamper M, Andreassen R, Stunt A (2011) Extreme cadmium and thallium isotope fractionations in enstatite chondrites. *Meteor Planet Sci* 46:A183–A183
- Palk C et al (2018) Variable Tl, Pb, and Cd concentrations and isotope compositions of enstatite and ordinary chondrites evidence for volatile element mobilization and decay of extinct Pb-205. *Meteor Planet Sci* 53:167–186
- Palme HHSCON (2014) Treatise on geochemistry (Second Edition). 3.1-Cosmochemical estimates of mantle composition reference module in earth systems and environmental sciences, vol 3, pp 1–39
- Peacock CL, Moon EM (2012) Oxidative scavenging of thallium by birnessite: explanation for thallium enrichment and stable isotope fractionation in marine ferromanganese precipitates. *Geochim Cosmochim Acta* 84:297–313
- Pengra JG, Genz H, Fink RW (1978) Orbital electron-capture ratios in decay of Pb-205. *Nucl Phys A* 302:1–11
- Piilonen PC, McDonald AM, Lalonde AE (2003) Insights into astrophyllite-group minerals II: crystal chemistry. *Can Miner* 41:27–54
- Rader ST, Mazdab FK, Barton MD (2018) Mineralogical thallium geochemistry and isotope variations from igneous, metamorphic, and metasomatic systems. *Geochim Cosmochim Acta* 243:42–65
- Rehkamper M, Halliday AN (1999) The precise measurement of Tl isotopic compositions by MC-ICPMS: application to the analysis of geological materials and meteorites. *Geochim Cosmochim Acta* 63:935–944
- Rehkamper M, Frank M, Hein JR, Porcelli D, Halliday A, Ingri J, Liebetrau V (2002) Thallium isotope variations in seawater and hydrogenetic, diagenetic, and hydrothermal ferromanganese deposits. *Earth Planet Sci Lett* 197:65–81
- Richardson SM, Richardson JW (1982) Crystal structure of a pink muscovite from Archer's Post, Kenya: implications for reverse pleochroism in dioctahedral micas. *Am Miner* 67:69–75
- Sabrowsky H (1971) Zur Darstellung und Kristallstruktur von  $Tl_2O$ . *Z Anorg Allg Chem* 381:266–278
- Salters VJM, Stracke A (2004) Composition of the depleted mantle. *Geochem Geophys Geosyst* 5
- Schauble EA (2007) Role of nuclear volume in driving equilibrium stable isotope fractionation of mercury, thallium, and other very heavy elements. *Geochim Cosmochim Acta* 71:2170–2189
- Schauble EA (2013) Modeling nuclear volume isotope effects in crystals. *Proc Natl Acad Sci USA* 110:17714–17719
- Schneider A, Heymer G (1956) Die Temperaturabhängigkeit der Molvolumina der Phasen Na Tl und Li Cd. *Z Anorg Allg Chem* 286:118–135
- Shaw DM (1952) The geochemistry of thallium. *Geochim Cosmochim Acta* 2:118–154
- Taylor WH (1934) The structure of sanidine and other feldspars. *Z Kristallogr Kristallgeom Kristallphys Kristallchem* 87:464–481
- Urey HC (1947) The thermodynamic properties of isotopic substances. *J Chem Soc* 5:562–581
- Velde G, Baerends EJ (1991) Precise density-functional method for periodic structures. *Phys Rev B* 44:7888
- Velde G, Bickelhaupt FM, Gisbergen SJA, Guerra C, Baerends EJ, Snijders JG, Ziegler T (2001) Chemistry with ADF. *J Comput Chem* 22:931
- Viswanathan K, Kielhorn HM (1983) Al, Si distribution in a ternary (Ba, K, Na)-feldspar as determined by crystal structure refinement. *Am Miner* 68:122–124
- Walker RJ (2014) Siderophile element constraints on the origin of the Moon. *Philos Trans R Soc Math Phys Eng Sci* 2024:1–13
- Wood BJ, Nielsen SG, Rehkamper M, Halliday AN (2008) The effects of core formation on the Pb- and Tl-isotopic composition of the silicate Earth. *Earth Planet Sci Lett* 269:325–335
- Yang S, Liu Y (2015) Nuclear volume effects in equilibrium stable isotope fractionations of mercury, thallium and lead. *Sci Rep* 5:12626
- Yang S, Liu Y (2016) Nuclear field shift effects on stable isotope fractionation: a review. *Acta Geochim* 35:227–239
- Yokoi K, Takahashi K, Arnould M (1985) The production and survival of Pb-205 in stars, and the Pb-205-Tl-205s-process chronometry. *Astron Astrophys* 145:339–346
- Zaccarini F, Thalhammer O, Princivalle F, Lenaz D, Stanley C, Garuti G (2007) Djerfisherite in the Guli dunite complex, Polar Siberia: A primary or metasomatic phase? *Can Miner* 45:1201–1211